

Fatigue crack propagation micromechanisms in a ferritic and in a ferritic-pearlitic ductile cast iron

F. Iacoviello^{1, a}, V. Di Cocco^{1, b} and F. Franzese^{1, c}

¹Università di Cassino – Di.M.S.A.T., via G. Di Biasio 43, 03043 Cassino (FR) Italy

^aiacoviello@unicas.it, ^bv.dicocco@unicas.it, ^cf.franzese@unicas.it

Keywords: ductile iron, fatigue crack propagation.

Abstract. Ductile iron discovery in 1948 gave a new lease on life to the cast iron family. In fact these cast irons (DCIs) combine the good castability of gray irons and high toughness values of steels. Ductile cast irons are also characterized by high fatigue crack propagation resistance, although this property is still not widely investigated.

In the present work we considered two different ductile cast irons. The first was characterized by a fully ferritic matrix. The second was characterized by a ferritic-pearlitic matrix obtained annealing a fully pearlitic DCI. Their fatigue crack propagation resistance was investigated in air by means of fatigue crack propagation tests according to ASTM E647 standard, considering three different stress ratios ($R = K_{\min}/K_{\max} = 0.1; 0.5; 0.75$). Crack propagation micromechanisms were extensively analysed by means of a scanning electron microscope (SEM) both considering “a step by step” SEM lateral surface specimen observation and performing a traditional SEM fracture surface analysis, mainly focusing graphite nodules damaging micromechanisms and, obviously, considering microstructure influence.

Introduction

Because of their high strength, high toughness, good machinability, and low cost, ductile cast irons (DCIs) are widely used in the critical automotive parts as crankshafts, truck axles, etc. [1]. DCIs mechanical properties are directly related to their matrix microstructure (Fig. 1). Ferritic ductile irons are characterized by good ductility and a tensile strength that is equivalent to a low carbon steel. Pearlitic ductile irons shows high strength, good wear resistance and moderate ductility. Ferritic-pearlitic grades properties are intermediate between ferritic and pearlitic ones. Martensitic ductile irons show very high strength, but low levels of toughness and ductility. Bainitic grades are characterized by a high hardness. Austenitic ductile irons show good corrosion resistance, good strength and dimensional stability at high temperature. Austempered grades show a very high wear resistance and fatigue strength [2,3]. Their versatility is especially evident in the area of mechanical properties where ductile cast irons offer to designers the option of choosing high ductility (up to 18% elongation), or high strength, with tensile strengths exceeding 825 MPa. Austempered ductile iron offers even greater mechanical properties and wear resistance, providing tensile strengths exceeding 1600 MPa.

Considering graphite elements shape, a very high *nodularity* is strongly recommended. The peculiar morphology of graphite elements in ductile irons is responsible of DCIs good ductility and toughness. Characterized by a rough spherical shape, graphite particles contained in ductile irons are also known as “nodules”. They act as “crack arresters”, with a consequent increase of toughness, ductility and crack propagation resistance. DCIs fatigue crack propagation resistance has been found to be dependent on the microstructure, graphite nodules size and volume fraction, graphite elements shape and the chemical composition [4]. Graphite spheroids increase the importance of crack closure effect, with a strong microstructure influence [5]. Considering fully ferritic or fully pearlitic ductile irons, graphite elements debonding is an important crack closure mechanism (Fig. 2): higher ductile deformation corresponds to lower crack growth rates. Ferritic-pearlitic or bainitic-ferritic

microstructure are characterized by a similar phases distribution with a pearlitic or bainitic matrix and ferritic shields around graphite elements (more evident in ferritic-pearlitic ductile iron). Considering that both pearlite and bainite are characterized by a reduced ductility and higher UTS (Ultimate tensile strength) values, if compared to ferrite, a second peculiar closure effect due to the different mechanical behaviour of ferritic shields and of pearlitic or bainitic matrix was proposed. During the loading cycle, the ferrite and pearlite (or bainite) deformation level could be really different, especially corresponding to higher R and ΔK values:

- corresponding to K_{max} values, ferritic shields are more deformed than pearlitic (or bainitic) matrix;
- corresponding to K_{min} values, pearlitic (or bainitic) matrix induces on ferritic shields a residual compression stress condition with a consequent enhancing of the closure effect.

Microstructure and stress ratio influence on fatigue crack propagation resistance is shown in Fig. 3.

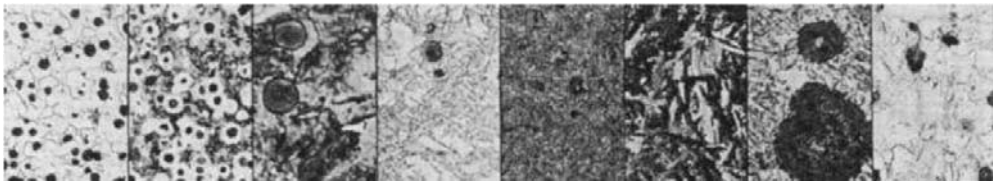


Fig. 1: Different DCIs microstructures. From left to right, respectively (different magnifications): ferritic, ferritic pearlitic, fully pearlitic, martensitic, tempered martensitic, austempered (UTS = 1050 MPa), austempered (UTS = 1600 MPa), austenitic [2].

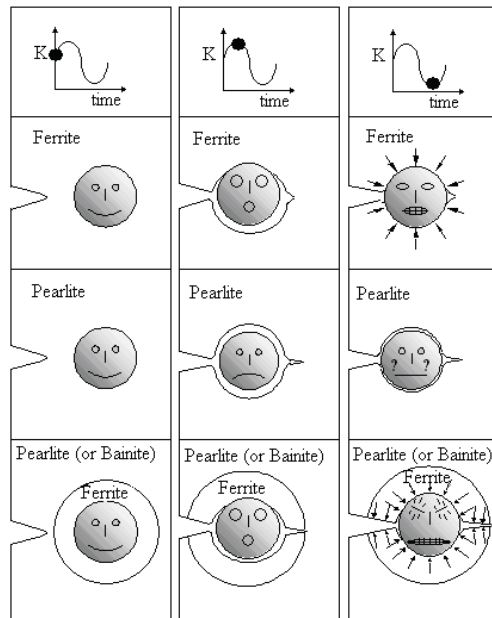


Fig. 2: Ductile and fragile graphite elements debonding influence on crack closure effect in ductile irons [5].

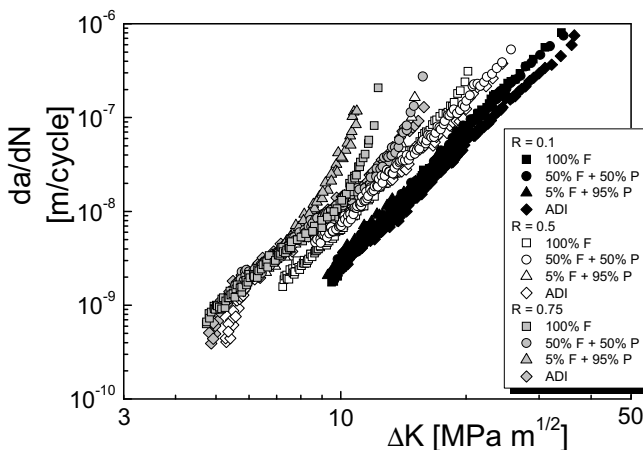


Fig. 3: Microstructure and stress ratio influence on fatigue crack propagation resistance [5].

In this work, two different DCIs were investigated considering three different stress ratios (R = 0.1; 0.5; 0.75). Crack propagation micromechanisms were investigated both by means of a scanning electron microscope (SEM) observation of fatigue crack propagation profiles (“step by step” analysis), and performing a traditional SEM fracture surface analysis.

Material and experimental procedure

Investigated DCI chemical composition are shown in tables 1 and 2. The first is an almost fully ferritic DCI. The second is a ferritic-pearlitic DCI obtained annealing an almost fully pearlitic DCI (final microstructure is in Fig. 4; 50% ferrite – 50% pearlite). It is evident that ferrite and pearlite distribution is quite different if compared to a ferritic-pearlitic ductile iron with an analogous phases volume fraction [5], but obtained by means of chemical composition control (Fig. 5; fatigue crack propagation resistance is in Fig. 3). Both the investigated ferritic-pearlitic DCIs are characterized by a very high graphite elements nodularity.

| C | Si | Mn | S | P | Cu | Cr | Mg | Sn |
|------|------|------|-------|-------|-------|-------|-------|-------|
| 3.62 | 2.72 | 0.19 | 0.011 | 0.021 | 0.019 | 0.031 | 0.047 | 0.011 |

Table 2. Investigated fully ferritic DCI chemical composition.

| C | Si | Mn | S | P | Cu | Cr | Mg | Sn |
|------|------|------|-------|-------|------|-------|-------|-------|
| 3.59 | 2.65 | 0.19 | 0.012 | 0.028 | 0,04 | 0.061 | 0.060 | 0.098 |

Table 2. Investigated ferritic-pearlitic DCI chemical composition.

Fatigue crack propagation tests were run according to ASTM E647 standard [6], using 10 mm thick CT (Compact Type) specimens and considering three different stress ratio values (e.g. $R = P_{\min}/P_{\max} = 0.1; 0.5; 0.75$). Tests were performed using a computer controlled INSTRON 8501 servohydraulic machine in constant load amplitude conditions, considering a 20 Hz loading frequency, a sinusoidal loading waveform and laboratory conditions. Crack length measurements were performed by means of a compliance method using a double cantilever mouth gage and controlled using an optical microscope (x40).

In order to analyze damage evolution during fatigue crack propagation, specimens lateral surfaces were previously metallographically prepared. During fatigue crack propagation tests, SEM crack path observations were performed corresponding to three different crack lengths. Furthermore, fracture surfaces were analyzed by means of a scanning electron microscope (cracks propagate from left to right).

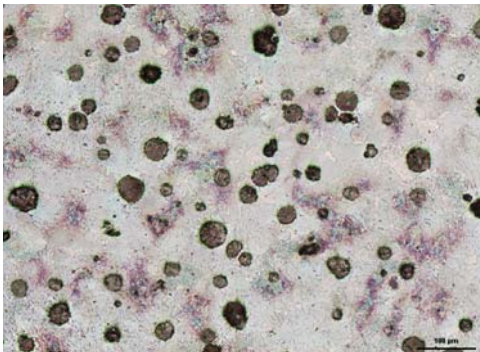


Fig. 4: Investigated DCI microstructure (after annealing; Nital 3).

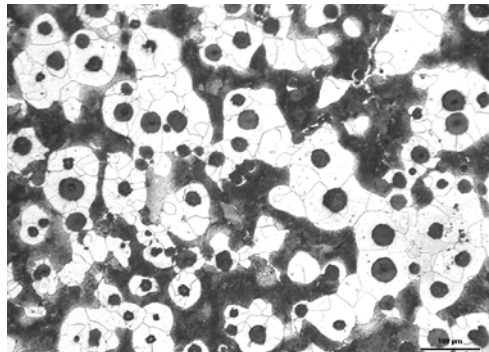


Fig. 5: Phases distribution in a ferritic-pearlitic ductile iron (obtained by means of chemical composition control; Nital 3).

Experimental results

Microstructure influence on fatigue crack propagation resistance is shown in Fig 6. Ferritic-pearlitic DCI, obtained annealing a fully pearlitic DCI, is characterized by a lower fatigue crack propagation resistance (lower crack growth rates for the same applied ΔK values) if compared to the ferritic-pearlitic DCI obtained by means of a chemical composition control (Fig.3). This is more evident in stage I of III (threshold stage, although no threshold tests were performed) and stage III of III (final rupture stage). Focusing stage II of III (Paris stage), differences between investigated DCIs are really low. As a consequence of the reduce fatigue crack propagation resistance of ferritic-pearlitic DCI, differences between the DCI investigated in this work are low [Fig. 6].

Ferritic-pearlitic DCI obtained by means of an annealing heat treatment crack profile analysis showed different damaging micromechanisms: crack branching (Fig. 7), graphite nodules debonding and cracking (Figs. 8 and 9, respectively). Focusing crack tip zone, neither graphite nodules nor matrix seems to be damaged, also considering more critical loading conditions (higher ΔK and/or R values, Fig. 10).

Ferritic DCI is characterized by a lower importance of crack branching (Fig. 11). Graphite nodules debonding and cracking is evident (Figs. 11 and 12, respectively) and secondary cracks both in ferritic matrix and in graphite nodules are also observed near main crack (Figs. 13 and 14). Cracks in ferritic matrix seem to be due to the presence of graphite nodules near the specimens surface (Fig. 13). Due to this secondary damage micromechanism, fatigue crack propagation

resistance of ferritic DCI seems to be reduced. Different damaging micromechanisms in ferritic DCI are summarized in Fig 15.

SEM fracture surface analysis shows evident difference in crack propagation micromechanisms. Ferritic-pearlitic DCI is characterized by the presence of striations, with cleavage that is evident only considering more critical loading conditions (Fig. 16). Ferritic DCI is characterized by a more evident presence of cleavage on fracture surfaces, especially but not uniquely around graphite nodules (Fig. 17). Graphite nodule debonding is always ductile both in ferritic and in ferritic pearlitic DCI (Fig. 17).

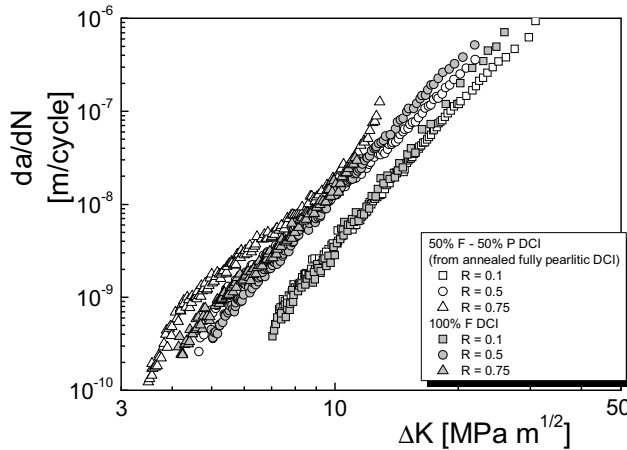


Fig. 6: Phases distribution and stress ratio influence on fatigue crack propagation resistance in 50%-50% ferritic-pearlitic DCIs with different phases distribution.

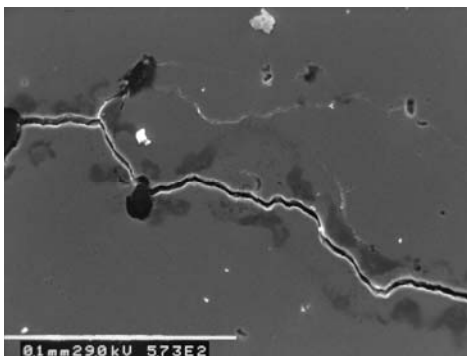


Fig. 7: Ferritic-pearlitic DCI. Crack branching ($R = 0.1$; $\Delta K = 10 MPa\sqrt{m}$).

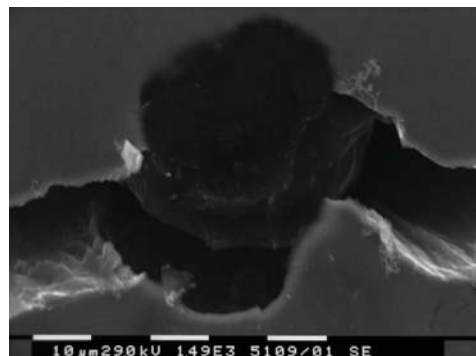


Fig. 8: Ferritic-pearlitic DCI. Graphite nodule debonding ($R = 0.75$; $\Delta K = 8 MPa\sqrt{m}$).

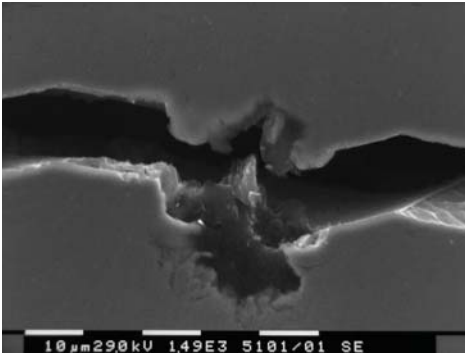


Fig. 9: Ferritic-pearlitic DCI. Graphite nodule cracking ($R = 0.5$; $\Delta K = 9 \text{ MPa}\sqrt{\text{m}}$).

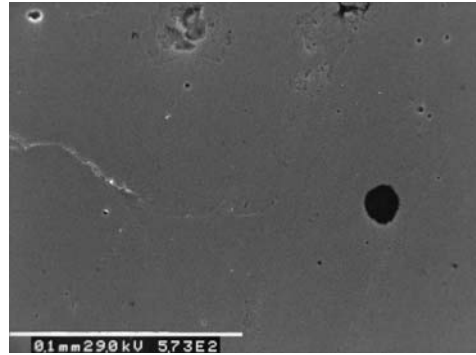


Fig. 10: Ferritic-pearlitic DCI. Damaging at crack tip ($R = 0.75$; $\Delta K = 11 \text{ MPa}\sqrt{\text{m}}$).

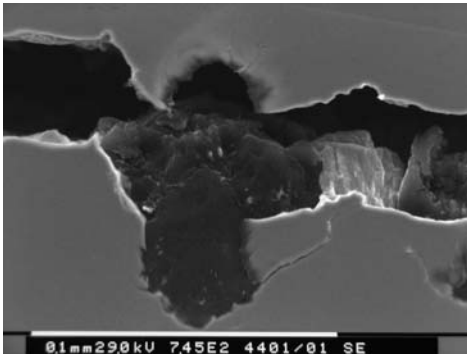


Fig. 11: Ferritic DCI. Crack branching and graphite nodule debonding ($R = 0.1$; $\Delta K = 10 \text{ MPa}\sqrt{\text{m}}$).

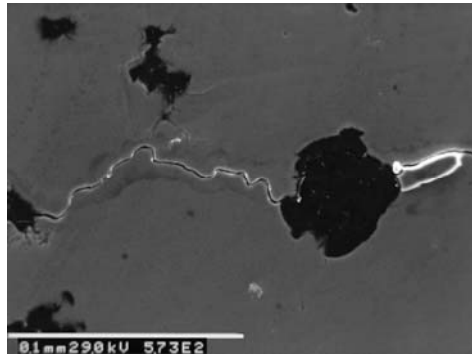


Fig. 12: Ferritic DCI. Graphite nodule cracking ($R = 0.5$; $\Delta K = 9 \text{ MPa}\sqrt{\text{m}}$).

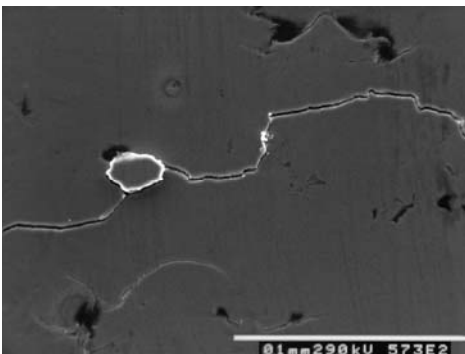


Fig. 13: Ferritic DCI. Secondary cracks near main crack ($R = 0.75$; $\Delta K = 8 \text{ MPa}\sqrt{\text{m}}$).

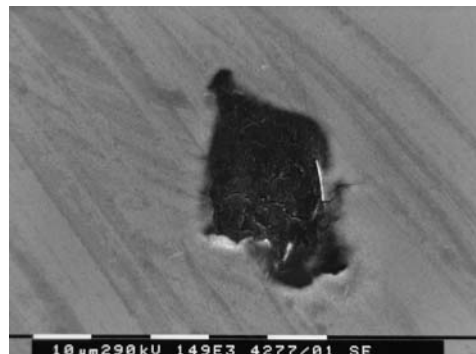


Fig. 14: Ferritic DCI. Secondary cracks in graphite nodules ($R = 0.75$; $\Delta K = 5 \text{ MPa}\sqrt{\text{m}}$).

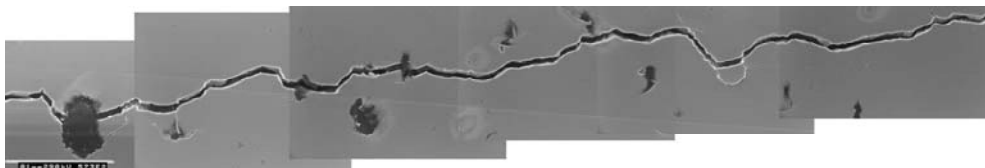


Fig. 15: Different damaging micromechanisms in ferritic DCI ($R = 0.75$; $\Delta K = 10-11 \text{ MPa}\sqrt{\text{m}}$).

Considering experimental results obtained in this work and the previous research activity concerning ferritic-pearlitic [5], graphite nodules ductile debonding is confirmed as an important crack propagation micromechanism, increasing the evidence of crack closure effect. Furthermore, DCI fatigue crack propagation resistance is strongly affected by matrix microstructure, considering both phases volume fraction and distribution. Finally, a secondary damaging micromechanism was observed in ferritic DCI as secondary cracks not connected with the main crack, both in ferritic matrix and in graphite nodules. This damaging micromechanism do not affect the main crack fatigue crack propagation resistance, but increase the damaging level in the specimen, also far from the main crack.

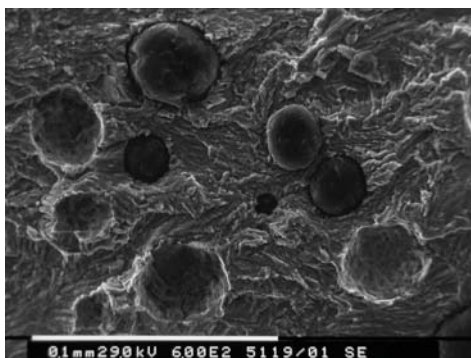


Fig. 16: Ferritic-pearlitic DCI fracture surface analysis. Striations and graphite nodules ductile debonding ($R = 0.75$; $\Delta K = 7 \text{ MPa}\sqrt{\text{m}}$).

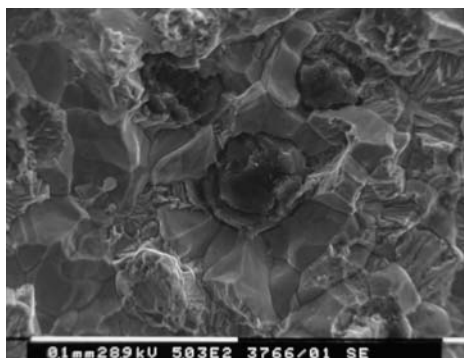


Fig. 17: Ferritic DCI fracture surface analysis. Cleavage ($R = 0.1$; $\Delta K = 13 \text{ MPa}\sqrt{\text{m}}$).

Conclusions

Ductile cast irons (DCIs) have significantly good combination of tensile strength, ductility and toughness, along with good wear resistance and hardenability. A variety of microstructures were recently developed, from fully ferritic to fully pearlitic, bainitic or martensitic one.

In this work, two DCIs were considered: a fully ferritic one, and a ferritic-pearlitic one (50% ferrite and 50% pearlite). Second DCI was obtained annealing a fully pearlitic DCI. Their fatigue crack propagation resistance was investigated in air by means of fatigue crack propagation tests according to ASTM E647 standard, considering three different stress ratios ($R = K_{\min}/K_{\max} = 0.1$; 0.5; 0.75). Crack propagation micromechanisms were extensively analysed by means of a scanning electron microscope (SEM) both considering “a step by step” SEM lateral surface specimen observation and performing a traditional SEM fracture surface analysis, mainly focusing graphite nodules damaging micromechanisms and, obviously, considering microstructure influence.

On the basis of the experimental results, the following conclusions can be summarized:

- DCI fatigue crack propagation resistance is strongly affected by matrix microstructure; both phases volume fraction and phase distribution should be optimized.

- Different fatigue damaging micromechanisms were identified. Some of these micromechanisms are connected to crack propagation (matrix cleavage; striations; graphite nodules ductile debonding; graphite nodules cracking).
- Graphite nodules ductile debonding is more frequent than graphite elements cracking: crack closure due to graphite elements debonding seems to be a really important crack closure mechanism and its importance is not dependant on the loading conditions (R and/or applied ΔK)
- Ferritic DCI is characterized by an additional damaging mechanism: secondary cracks both in ferritic matrix and in graphite nodules are observed; these cracks do not have an evident effect on main crack propagation (in $da/dN-\Delta K$ diagram), but increase the damaging level in the material.

References

- [1] L.R. Jeckins, R.D. Forrest, Ductile Iron, in Properties and selection: iron, steels and high performance alloys. ASM Handbook, Metal Park (OH) ASM International, Vol.1, p.35.
- [2] R.G. Ward, *An Introduction to the Physical Chemistry of Iron and Steel Making*, Arnold, London, (1962).
- [3] C. Labrecque, M. Gagne, Can. Metall. Quart. Vol. 37 (1998), p. 343.
- [4] M. Cavallini, O. Di Bartolomeo, F. Iacoviello "Fatigue damaging micromechanisms in ductile cast irons" Proceedings of *International Conference on Fatigue Crack Paths (CP2006)*, Parma 14-16 september 2006, n. 13.
- [5] M. Cavallini, O. Di Bartolomeo, F. Iacoviello, Engineering Fracture Mechanics, Vol.75 (2008), p.694.
- [6] ASTM Standard test Method for Measurements of fatigue crack growth rates (E647-93). Annual Book of ASTM Standards. 0301, American Society for Testing and Materials, 1993.